American Journal of Geophysics, Geochemistry and Geosystems
Vol. 4, No. 1, 2018, pp. 1-12
http://www.aiscience.org/journal/aj3g
ISSN: 2381-7143 (Print); ISSN: 2381-7151 (Online)

Euler Deconvolution and Forward and Inverse Modelling of Aeromagnetic Anomalies over Ogoja and Bansara Areas of Lower Benue Trough, Nigeria

Ugwu Chinenye Martha*, Ugwu Gabriel Zeruwa

Department of Industrial Physics, Enugu State University of Science and Technology, Enugu, Nigeria

Abstract

Qualitative and quantitative interpretations of aeromagnetic anomalies over Ogoja and Bansara areas of Anambra Basin, Lower Benue Trough of Nigeria were carried out using Euler deconvolution and forward and inverse modelling methods. The study area which covers an area of approximately 6050 km^2 lies within latitude 6°0'0" to 7°0'0" North and longitude 8°30'00" to 9°0'00" East. The regional anomaly was separated from the total magnetic intensity field to obtain the residual anomaly using first order polynomial fitting technique. The edges and causative bodies of the residual anomaly were also sharpened to reduce anomaly complexity as well as fault trend amplification using first, second and horizontal derivatives. The result of the study shows thick sedimentary depth that is sufficient for hydrocarbon accumulation. The 3D basement topography map of the study area shows a linear depression with the deepest sedimentary thickness obtained at the Southeastern region (Bansara area). This implies that the prospect for hydrocarbon accumulation will be higher in Bansara area than in Ogoja. The deepest depths obtained from the results of the Euler deconvolution and forward and inverse modelling of the aeromagnetic data are 4511m and 4654m respectively. The magnetic susceptibilities of the intrusive bodies modelled by forward and inverse modelling techniques suggest the presence of minerals such as graphite and cassiterite as well as rock bearing minerals like limestone, granite and marble.

Keywords

Euler Deconvolution, Forward and Inverse Modelling, Magnetic Anomaly, Sedimentary Thickness,
Intrusive Bodies and Hydrocarbon Potentials

Received: September 10, 2017 / Accepted: December 19, 2017 / Published online: May 18, 2018

1. Introduction

Airborne geophysical survey is an important aspect of modern geophysics that allows faster and usually cheaper coverage of large exploration area. Airborne magnetics has over the years gained great advances and successes in search for hidden ores and structures associated with the deposit of oil and gas, at least in reconnaissance survey. Magnetic method of prospecting depends on the potential field characteristics of the subsurface rocks. The method therefore seeks the anomalies arising from changes in the physical properties of the subsurface rocks. Rocks differ in their magnetic mineral content, hence the magnetic anomaly map allows a visualization of the geological structure of the upper crust in the subsurface particularly the spatial geometry of bodies of rock and the presence of faults and folds. The main purpose of magnetic survey is to detect rocks or minerals possessing unusual magnetic properties that reveal themselves by causing disturbances or anomalies in the

---

* Corresponding author
E-mail address: favourchinenye97@yahoo.com (U. C. Martha)

intensity of the earth's magnetic field.

Following the call for renewed search for hydrocarbons in other basins other than the Niger Delta basin, attention has been shifted to the Anambra basin and the Chad basin for hydrocarbon explorations. This is as a result of the current cut in oil and gas production from the Niger Delta basin occasioned by the persistent youth restiveness and the untold vandalism in oil and gas pipelines and equipment. The lower Benue Trough of the Anambra basin has been reported to hold hydrocarbon potential from aeromagnetic studies carried out in the area ([1-7]).

In the light of the successes of aeromagnetic surveys in the Lower Benue Trough using forward and inverse modelling techniques ([5, 8, 9]), this paper reports the result of interpretation of aeromagnetic data over Ogoja and Bansara areas of the lower Benue Trough using Euler deconvolution and forward and inverse modelling methods.

2. Geology of the Study Area

The study area is located within the lower Benue Trough of Nigeria. The area lies within latitude 6°0'0" to 7°0'0" North and longitude 8°30'00" to 9°0'00" East. It covers an area of approximately $6050 km^2$.

The lower Benue Trough is underlain by a thick sedimentary sequence deposited during the Cretaceous. The oldest sediments belong to the Asu River Group (Figure 1) which uncomfortably overlies the Precambrian basement complex that is made up of granitic and magmatic rocks. The Asu River Group whose type section outcrops near Abakaliki has an estimated thickness of 2000m and is of Albian age [10]. The Asu River group comprises of argillaceous sandy shale, laminated sandstone, micaceous sandstone and minor limestone with an interfingering of mafic volcanics [11]. The shales are fissile, highly fractured and are associated with pyroclastic rocks, especially around Abakaliki and Ezillo areas ([12-14]). Deposited on top of these Asu River Group sediments in the area were the upper Cretaceous sediments, comprising mostly the Ezeaku shale. The Ezeaku shale consists of nearly 1000m of calcareous flaggy shale and siltstone, thin sandy shaley limestone and calcareous sandstone [15]. They are Turonian in age and are overlain by younger sediments of the Awgu shale (Coniancian). The Awgu shale consists of marine fossilferous grey bluish shale, limestone and calcareous sandstone. The Awgu shale is overlain by Nkporo shale (Campanian) which is also marine and has sandstone members. A geological map of the study area is shown in Figure 1.

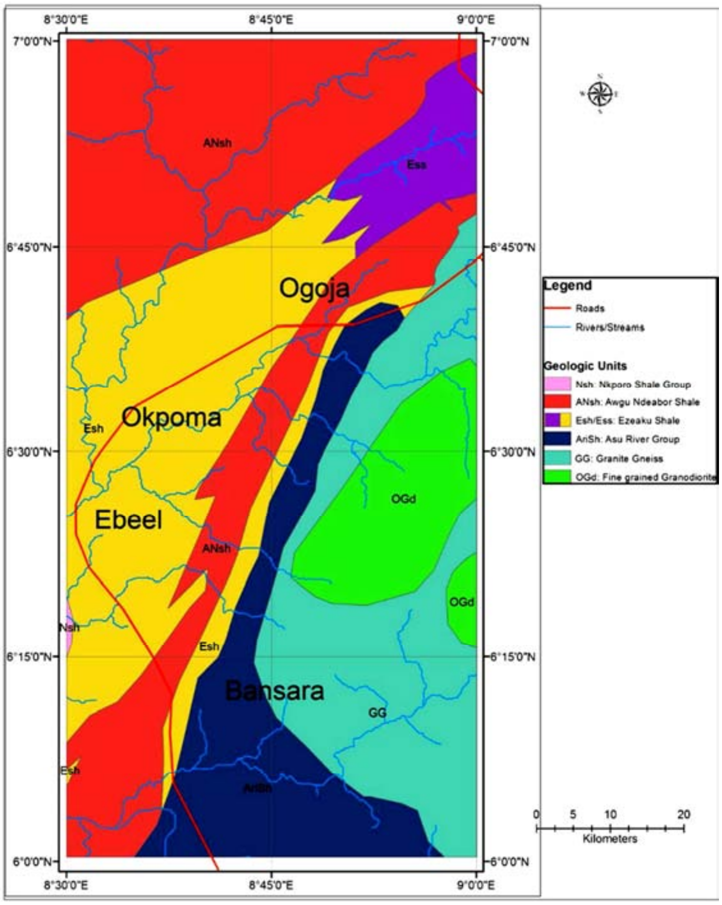

Figure 1. Geological map of the study area.

3. Materials and Methods

The materials used for this study include two sheets of aeromagnetic data of Ogoja and Bansara (sheets 290 and 304). Software applications used include Oasis Montaj, Wing Link, Potent Q 4.10.07 and Surfer 10. The high resolution aeromagnetic data of Ogoja (sheet 290) and Bansara (sheet 304) used for this study were obtained from the Nigerian Geological Survey Agency (NGSA). Fugro Airborne Surveys carried out the airborne geophysical work in 2009. The survey was flown at 80m elevation along flight lines spaced 500m apart. The flight line direction was 135° while the tie line direction was 225°.

The two digitized sheets were merged into a single sheet which formed the study area (Figure 2). The first step taken in reduction of the data was the polynomial fitting in order to remove the regional anomalies from the total magnetic intensity to obtain the residual anomaly (Figure 3). Different orders of polynomial were tried but we found the first order polynomial fitting to be the best for our data as it reflected the geological information of the study area.

Other data reduction techniques carried out on the residual intensity map include the calculation of the First Vertical Derivatives, Second Vertical Derivatives and Horizontal Derivatives.

The acquired data was quantitatively interpreted using Euler deconvolution and forward and inverse modelling techniques.

The data were interpreted using Euler deconvolution method to locate the source of potential field based on both amplitude and gradients. Employing the Euler deconvolution method, the Oasis Montaj software was applied on the Euler's homogeneity equation [16]:

$$(x - x_o)\frac{\partial M}{\partial x} + (y - y_o)\frac{\partial M}{\partial y} + (z - z_o)\frac{\partial M}{\partial z} = - NM \qquad (1)$$

where, $\frac{\partial M}{\partial x}$, $\frac{\partial M}{\partial y}$ and $\frac{\partial M}{\partial z}$ represent first order derivative of the magnetic field along x, y and z directions respectively. N is the structural index which is related to the geometry of the magnetic source. We used N = 3.0 for sphere, N = 2.0 for pipe, N = 1.0 for thin dyke and N = 0 for magnetic contact to calculate the shallow and deep depths. The base level of the regional magnetic field, B was computed using the equation [16]:

$$x_o\frac{\partial M}{\partial x} + y_o\frac{\partial M}{\partial y} + z_o\frac{\partial M}{\partial z} + NB = x\frac{\partial M}{\partial x} + y\frac{\partial M}{\partial y} + z\frac{\partial M}{\partial z} + NM \qquad (2)$$

The structural index (N) assigned to equations (1) and (2) helps in obtaining a system of linear equations and also in estimating the location and depth of the magnetic body.

The forward modelling technique being a trial and error method, the shape, position and physical properties of the model were adjusted in order to obtain a good correlation between the observed field and the calculated field data. The inverse modelling automatically adjusts model parameters to obtain a best fit between the observed and the calculated field. Potent Q 4.10.07 software was used for the modelling and inversion of the anomalies.

4. Results and Discussion

Figure 2 shows the total magnetic intensity (TMI) map of the study area. The map is presented as colour shades for easy interpretation. The colour shades aid the visibility of a wide range of anomalies in the magnetic map. The magnetic intensity ranges from -53.1nT (blue colour) to 100.7nT (pink colour). Areas of very strong magnetic susceptibility values (85.7nT to 100.7nT) are caused probably by near surface igneous or metamorphic rocks while the areas between -53.1nT and -3.3nT are most likely due to sedimentary rocks and other non-magnetic sources like sandstones.

The residual magnetic field was used to bring into focus local features which tend to be obscured by the broad features of the regional field. The residual magnetic field of the study area (Figure 3) was produced by removing the regional field from the total magnetic field using the polynomial fitting method. The 2D residual field ranges from -94.1nT (minimum) to 63.7nT (maximum). Generally, the entire study area revealed both positive and negative residual anomalies, indicating series of magnetic highs and lows. The positive residual anomalies could be related to the surface rocks (outcrops) and/or with measured magnetic values. The positive anomalies could also be interpreted in terms of combined effect of zones of intermediate intrusions occurring in the basement or within the sedimentary basin. Conversely, negative residual anomalies were depicted by definite magnetic lows. Figures 4, 5 and 6 show the First vertical derivative, Second vertical derivative and the Horizontal derivative map respectively after the data reductions. The horizontal derivative enhancement technique was applied on the residual intensity field to reveal subtle geophysical features. The horizontal derivative map shows the occurrence of subsurface linear structures which suggest the presence of fault in the area.

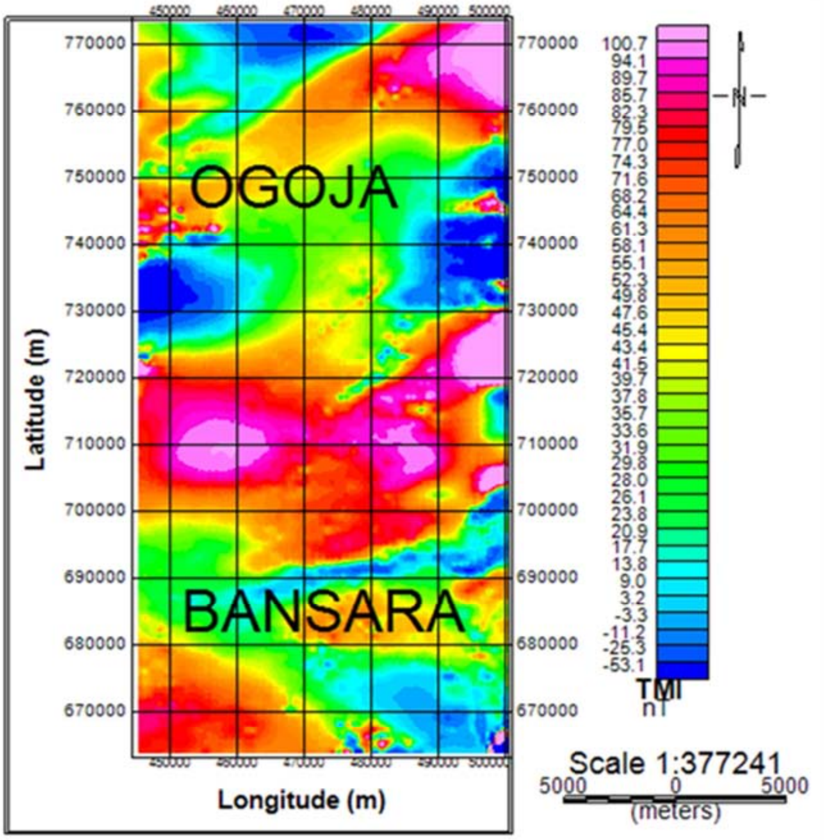

Figure 2. TMI map of the study area.

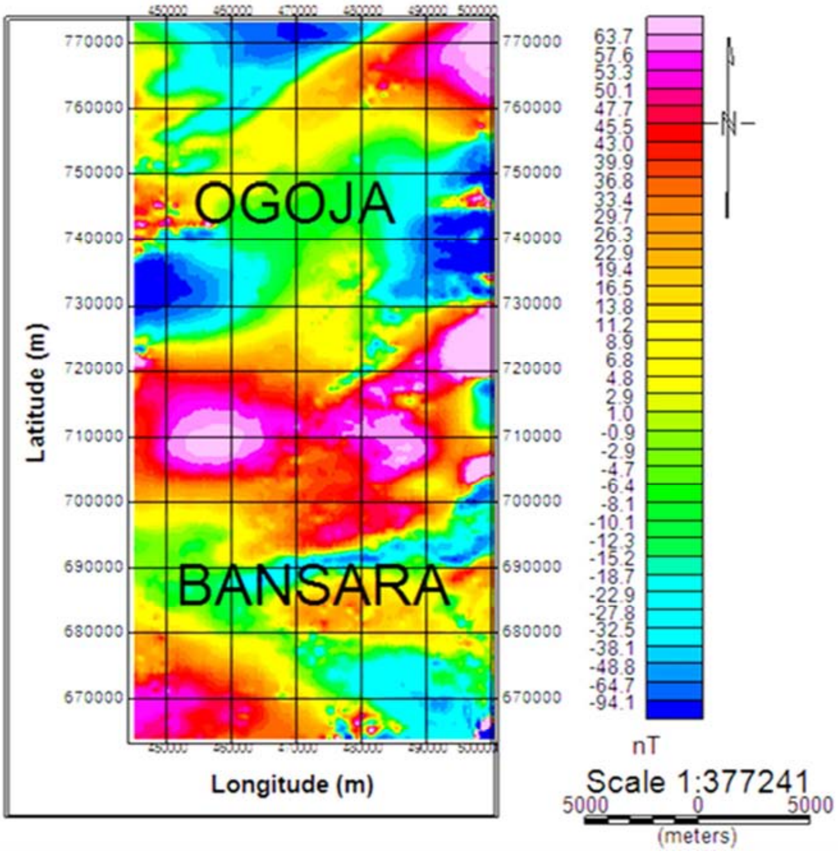

Figure 3. Residual anomaly map of the study area.

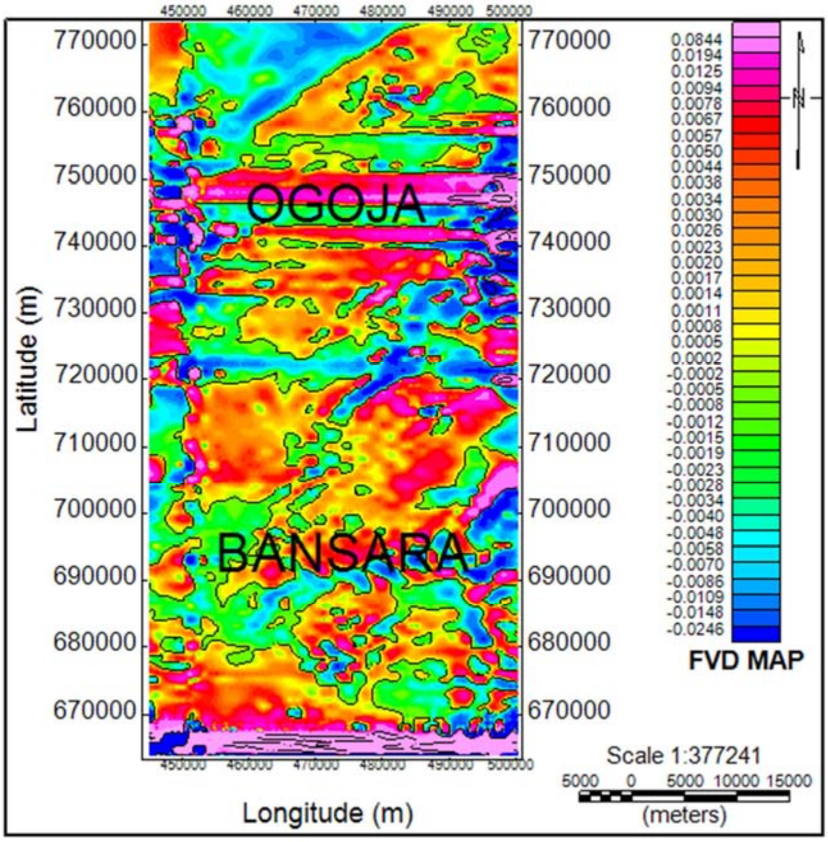

Figure 4. First vertical derivative map of the study area.

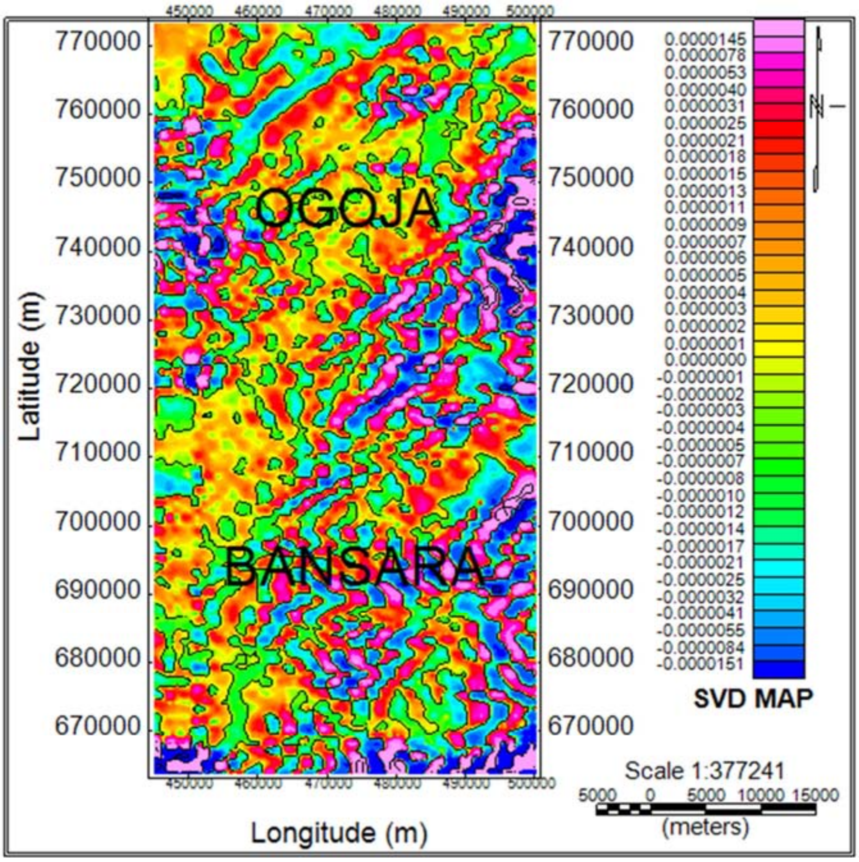

Figure 5. Second vertical derivative map of the study area.

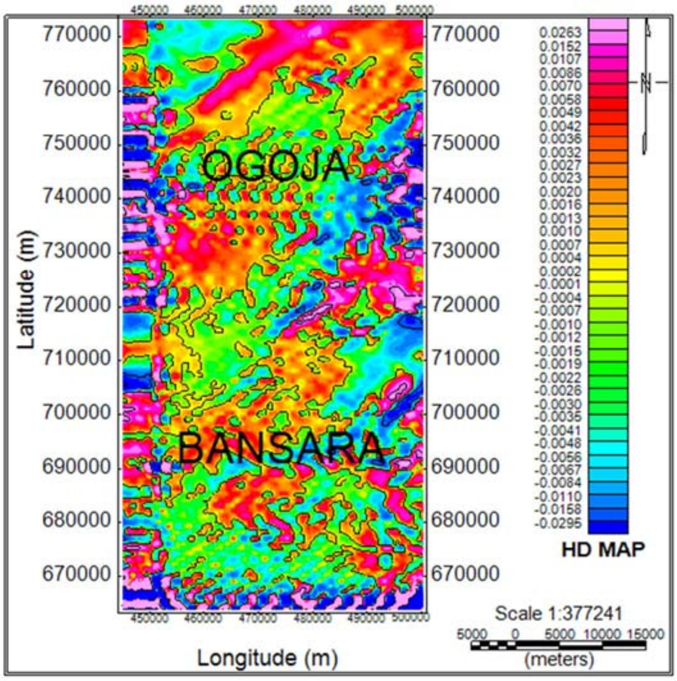

Figure 6. Horizontal derivative map of the study area.

In computing the Euler depths, standard Euler deconvolution interpretation was carried out in three dimensions, employing Oasis montaj software. The Euler depths were estimated using vertical derivatives in three dimensions (x, y and z). Hence, depths of shallow magnetic bodies or anomalies for different structural indices were displayed by Euler method. For five different structural indices (SI = 0.0, 0.5, 1.0, 2.0, 3.0), five Euler deconvolution maps were generated as shown in Figures 7-11. The pink colour indicates shallow magnetic bodies while the blue colour indicates deep lying magnetic bodies. The result of Euler deconvolution shows that the depth of horizontal contact body ranges from 357.0 to -834.9m for SI = 0.0; depth of vertical contact ranges from 520.8 to -1640.5m for SI = 0.5; depth of top of a vertical dyke or the edge of a sill ranges from 559.3 to -2327.2m for SI = 1.0; depth of a vertical cylinder ranges from 291.5 to -3545.0m for SI = 2.0; and depth of magnetic sphere or dipole ranges from -120.5 to -4511m for SI = 3.0. The result of 3D Euler depths are summarized in Table 1.

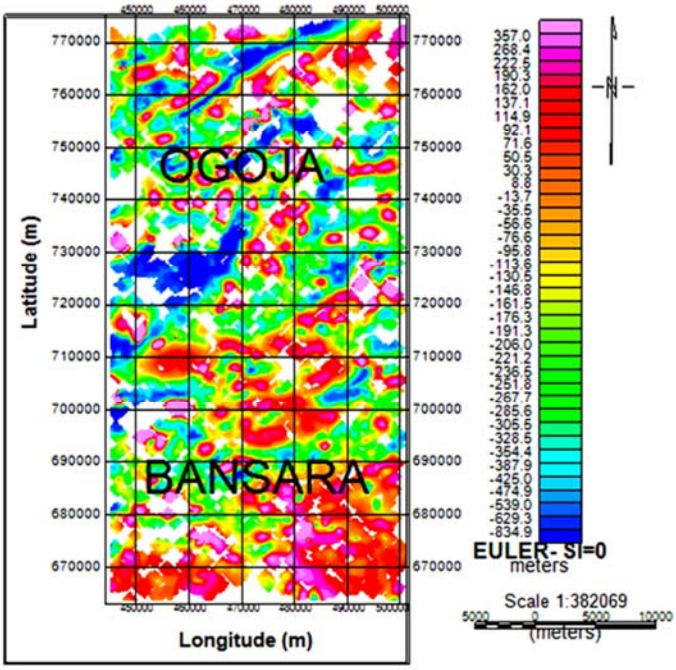

Figure 7. Euler - 2D map (SI = 0.0).

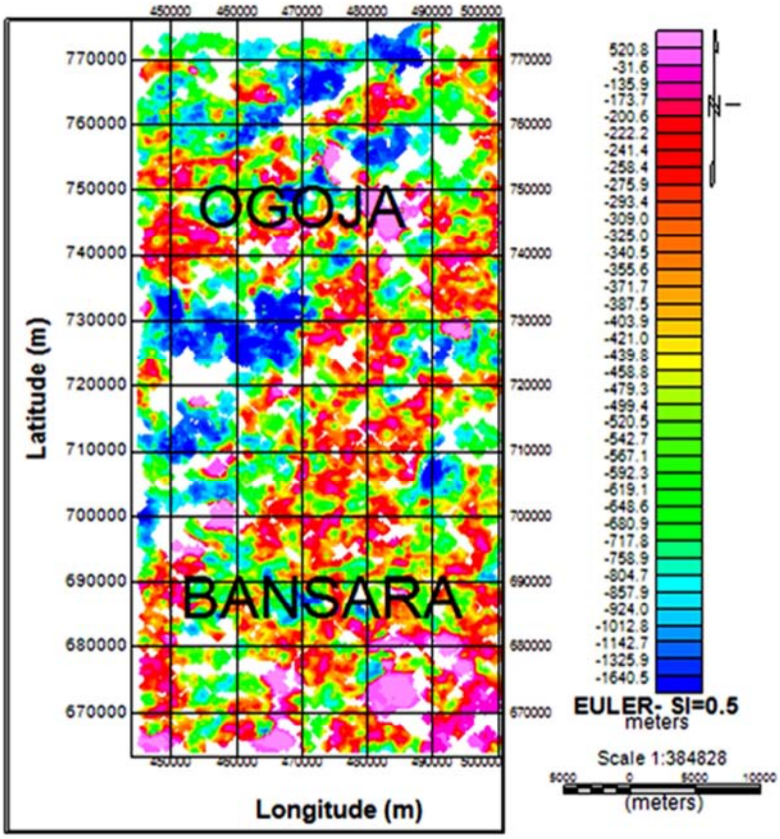

Figure 8. Euler - 2D map (SI = 0.5).

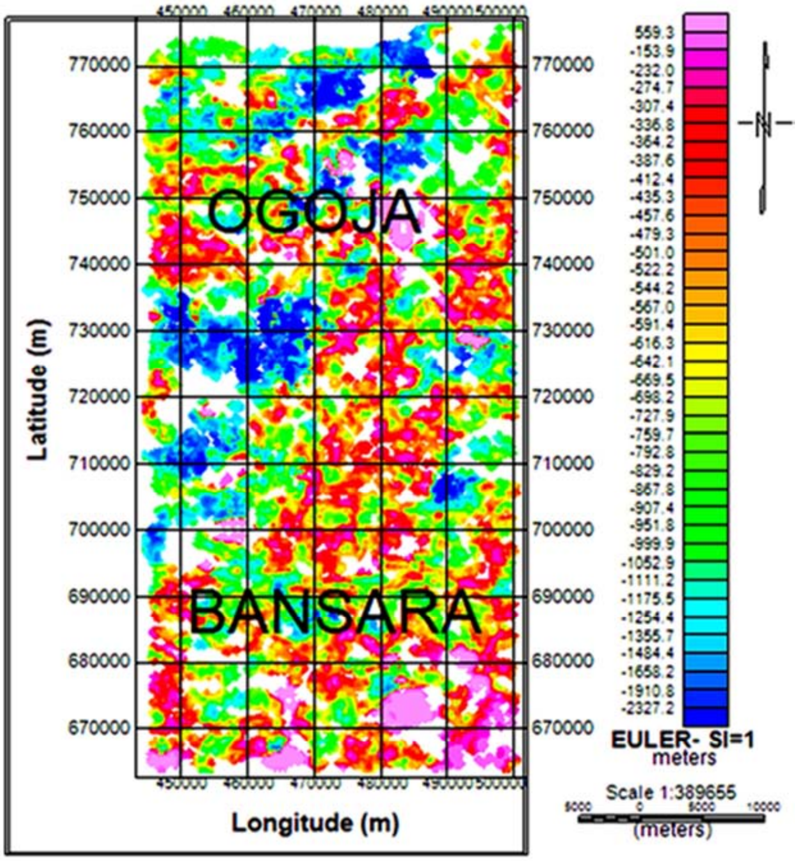

Figure 9. Euler - 2D map (SI = 1.0).

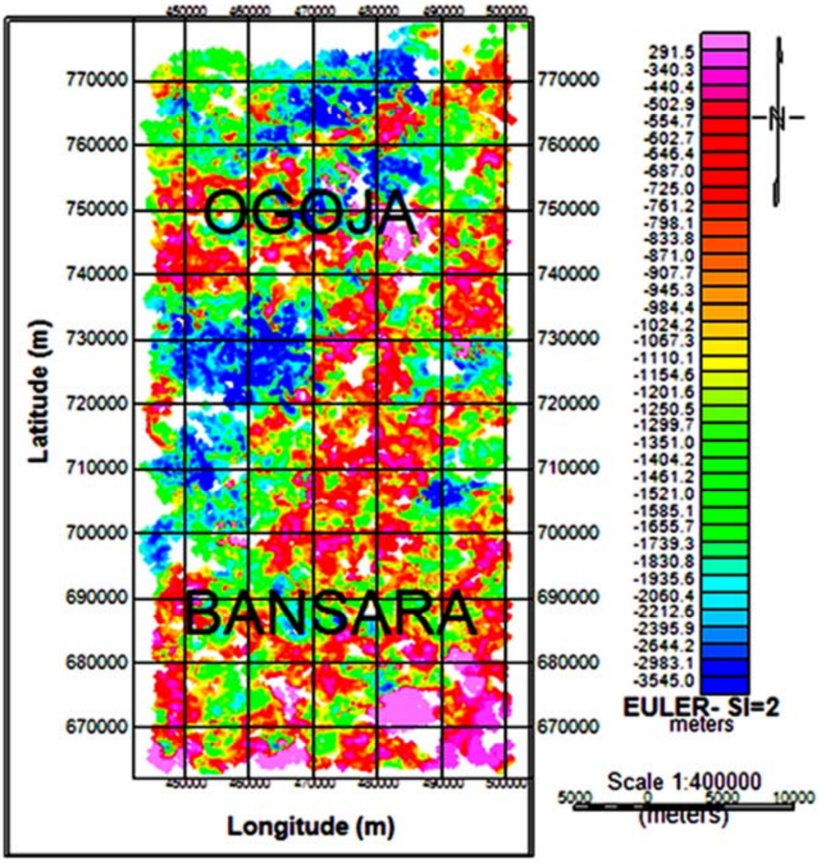

Figure 10. Euler 2D map (SI = 2.0).

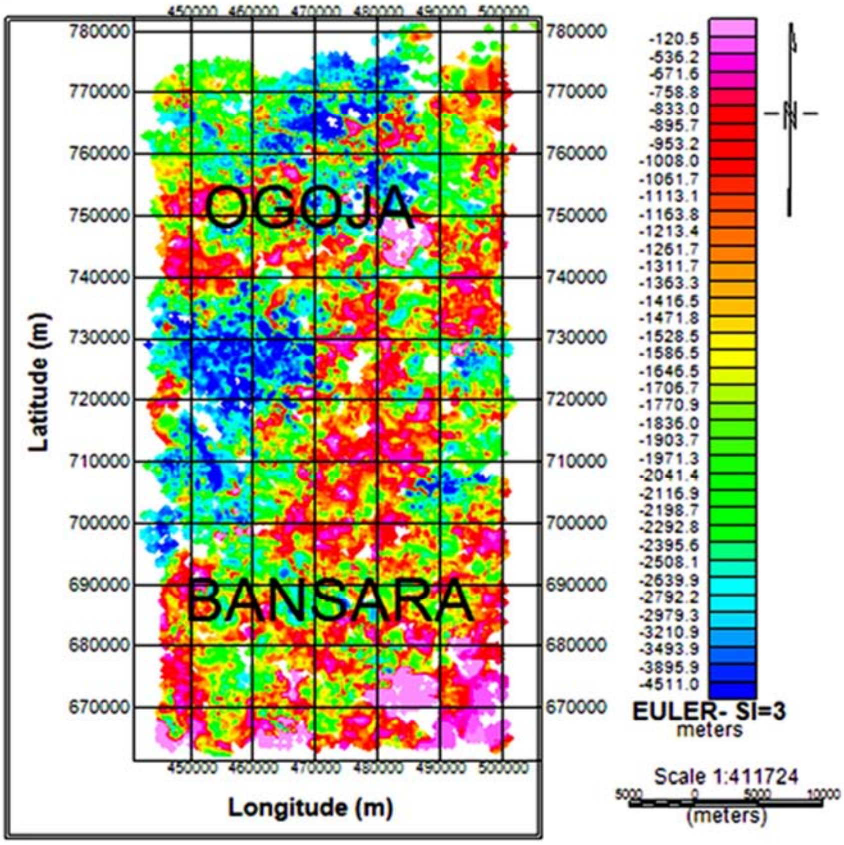

Figure 11. Euler-2D map (SI = 3.0).

Table 1. Summary of Euler depths determination.

Structural index, SI	Depth range (m)
0.0	From 357.0 to -834.9
0.5	From 520.8 to -1640.5
1.0	From 559.3 to -2327.2
2.0	From 291.5 to -3545.0
3.0	From -120.5 to -4511.0

In interpreting the magnetic anomalies in the area using forward and invers modelling techniques, five profiles were taken on the residual intensity grid of the study area (Figure 12). The model parameters are as shown in Figures 13-17. The magnetic susceptibility values obtained from profiles 1, 2, 3, 4 and 5 are 0.0400, 0.0001, 0.0250, 0.0003 and 0.0002 respectively; with respective depths of 4286m, 931m, 4654m, 2063m and 894m. The dominance of minerals like graphite and clay, as well as rock bearing minerals like limestone, granite and marble are indicated by their susceptibility values [17]. The results of the forward and inverse modelling techniques are summarized in Table 2.

The deepest depths obtained from Euler deconvolution (4511m) and forward and inverse modelling (4654m) show thick sediment that is sufficient for hydrocarbon accumulation.

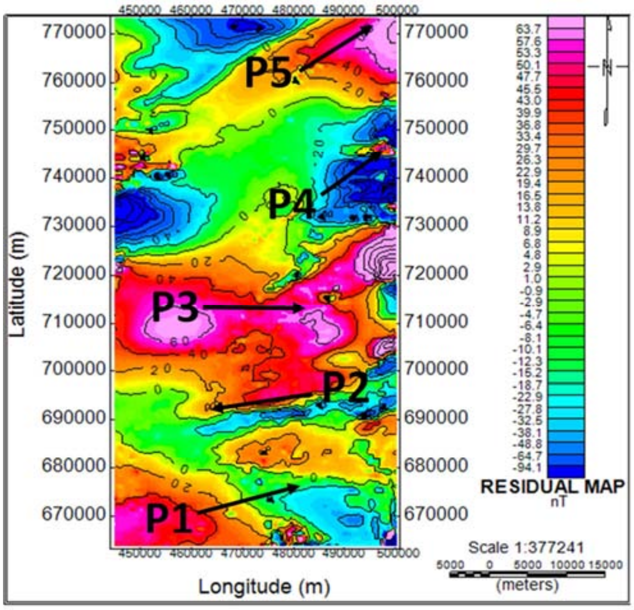

Figure 12. Profiles taken on the residual map of the study area.

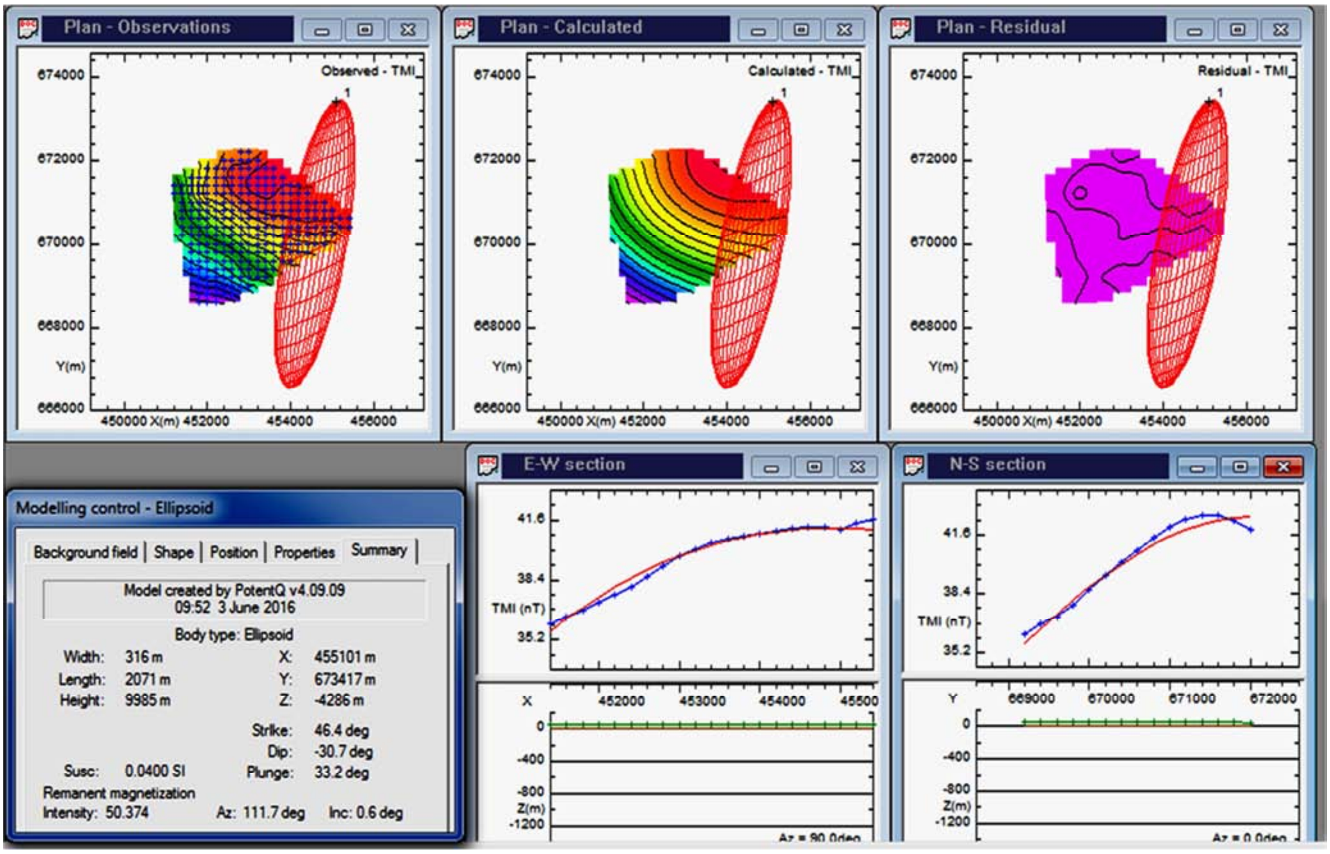

Model created by PotentQ v4.09.09
09:52 3 June 2016

Body type: Ellipsoid

Width: 316 m
Length: 2071 m
Height: 9985 m
X: 455101 m
Y: 673417 m
Z: -4286 m
Strike: 46.4 deg
Dip: -30.7 deg
Plunge: 33.2 deg
Susc: 0.0400 SI

Remanent magnetization
Intensity: 50.374
Az: 111.7 deg
Inc: 0.6 deg

Figure 13. Model result of profile 1 (P1).

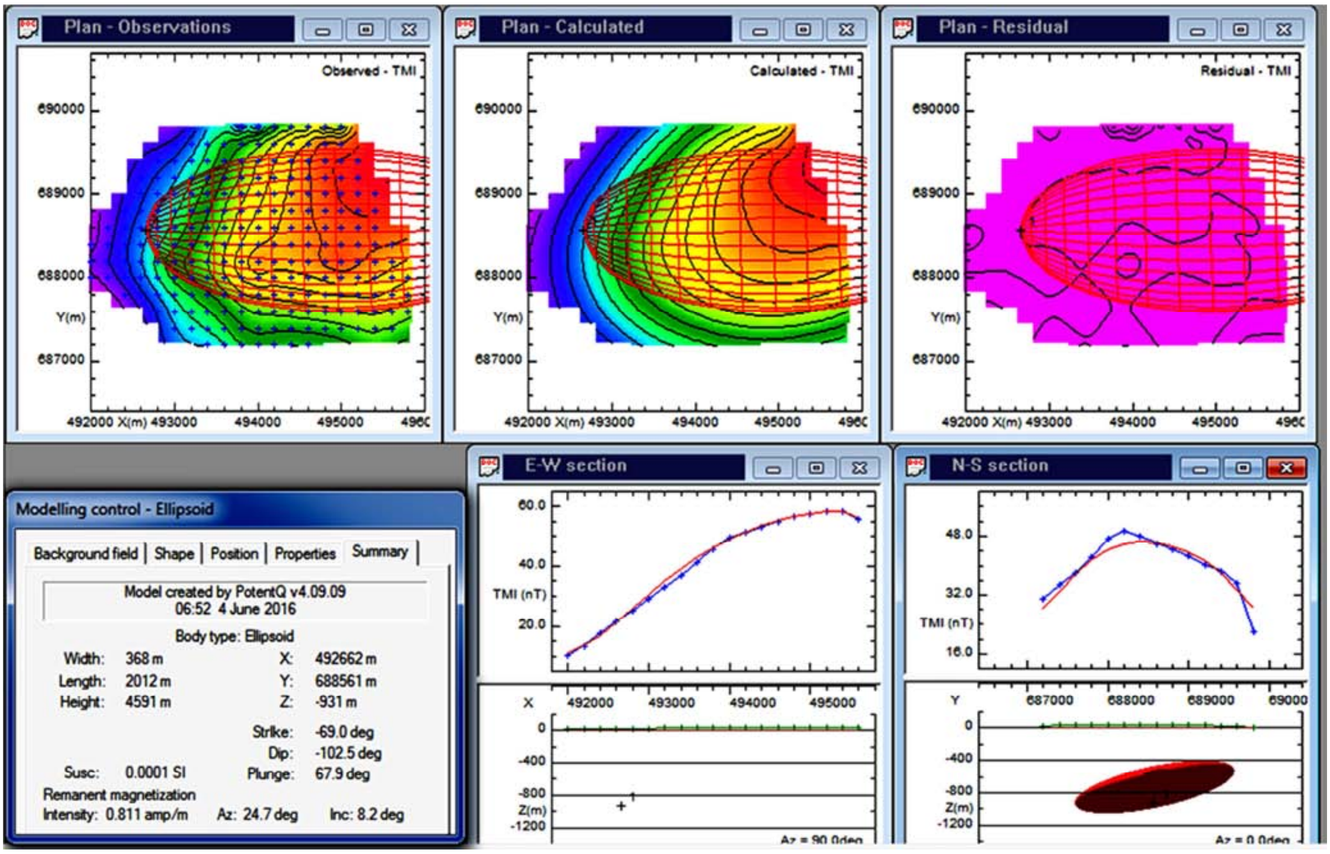

Model created by PotentQ v4.09.09
06:52 4 June 2016

Body type: Ellipsoid

Width: 368 m
Length: 2012 m
Height: 4591 m
X: 492662 m
Y: 688561 m
Z: -931 m
Strike: -69.0 deg
Dip: -102.5 deg
Susc: 0.0001 SI
Plunge: 67.9 deg
Remanent magnetization
Intensity: 0.811 amp/m Az: 24.7 deg Inc: 8.2 deg

Figure 14. Model result of profile 2 (P2).

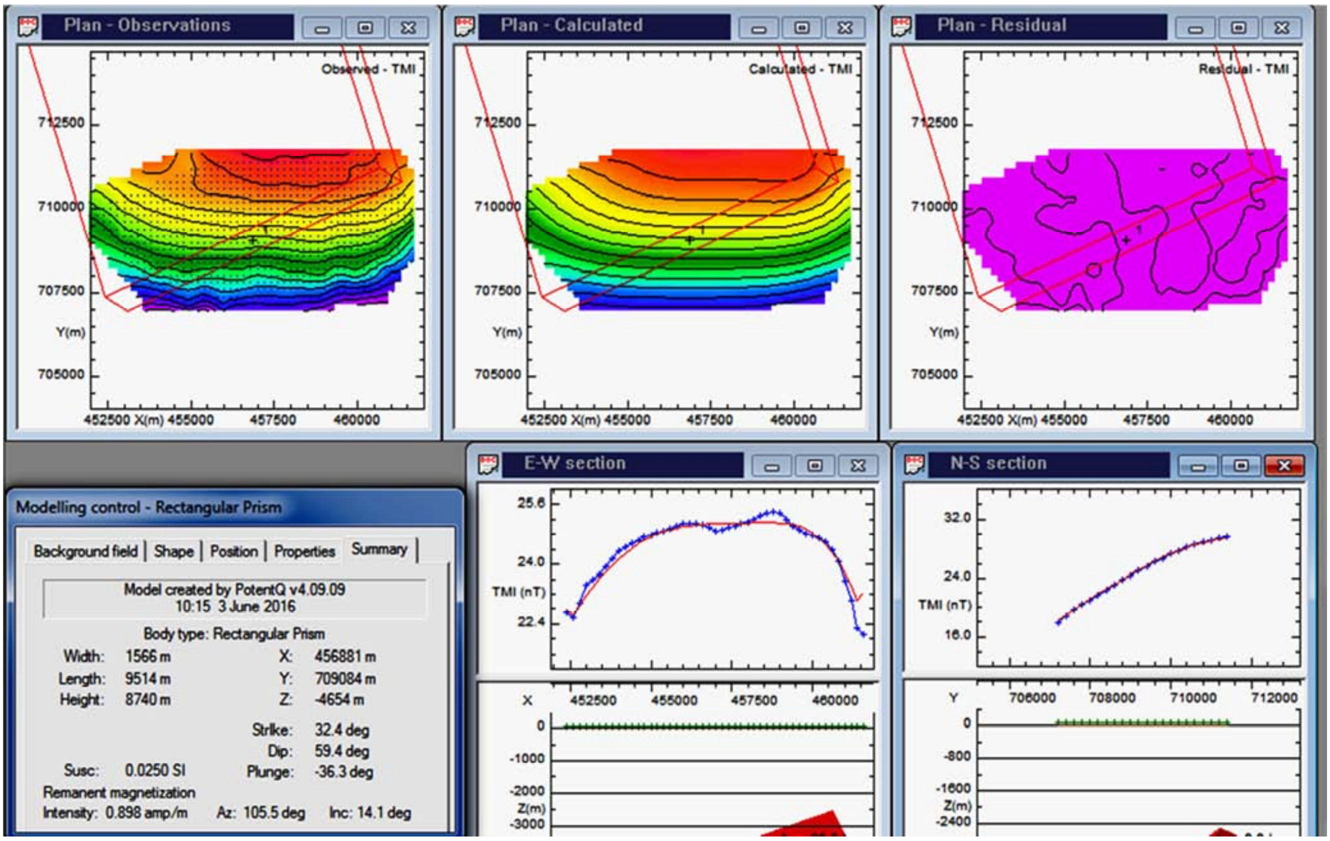

Model created by PotentQ v4.09.09
10:15 3 June 2016

Body type: Rectangular Prism

Width: 1566 m
Length: 9514 m
Height: 8740 m
X: 456881 m
Y: 709084 m
Z: -4654 m
Strike: 32.4 deg
Dip: 59.4 deg
Susc: 0.0250 SI
Plunge: -36.3 deg
Remanent magnetization
Intensity: 0.898 amp/m Az: 105.5 deg Inc: 14.1 deg

Figure 15. Model result of profile 3 (P3).

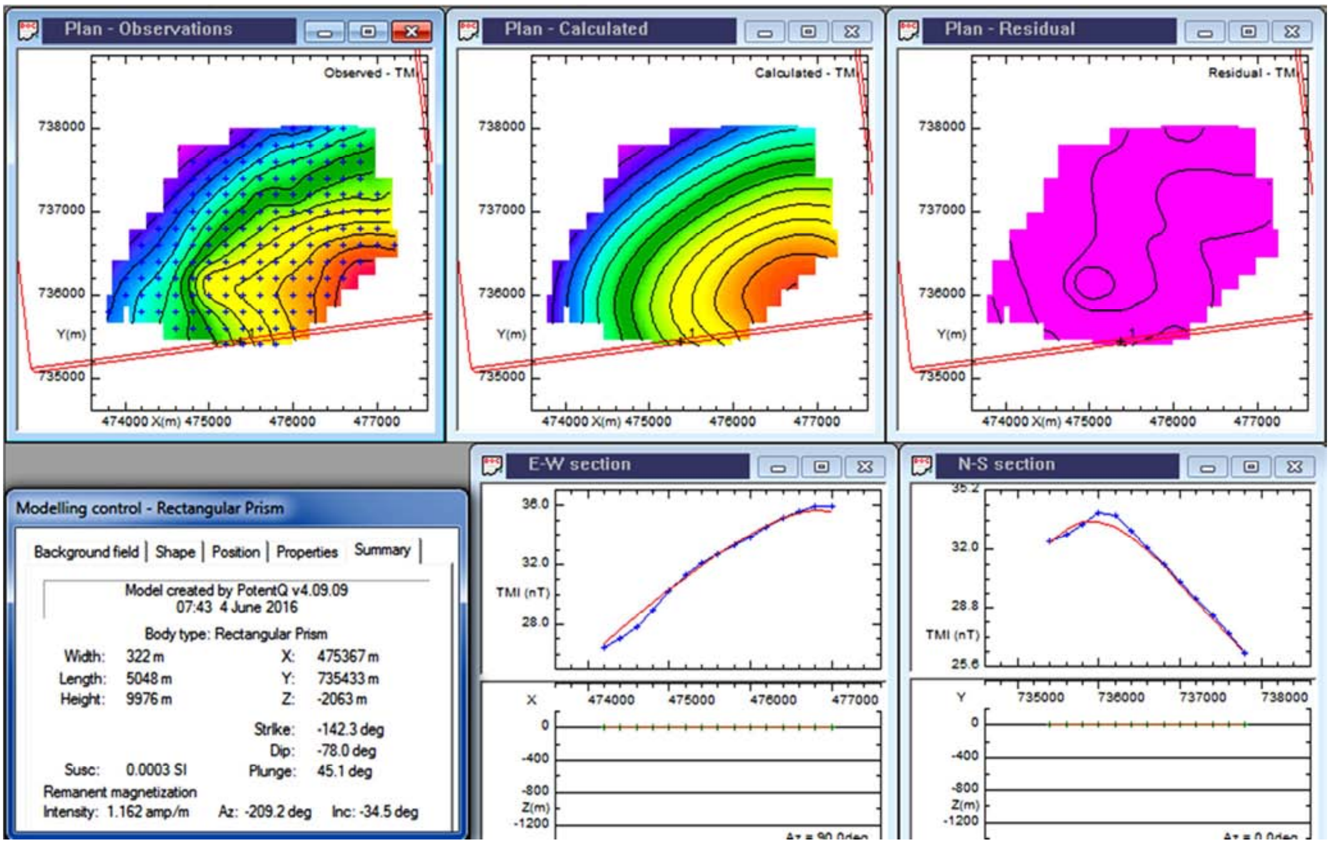

Model created by PotentQ v4.09.09
07:43 4 June 2016

Body type: Rectangular Prism

Width: 322 m
Length: 5048 m
Height: 9976 m
X: 475367 m
Y: 735433 m
Z: -2063 m
Strike: -142.3 deg
Dip: -78.0 deg
Susc: 0.0003 SI
Plunge: 45.1 deg
Remanent magnetization
Intensity: 1.162 amp/m
Az: -209.2 deg
Inc: -34.5 deg

Figure 16. Model result of profile 4 (P4).

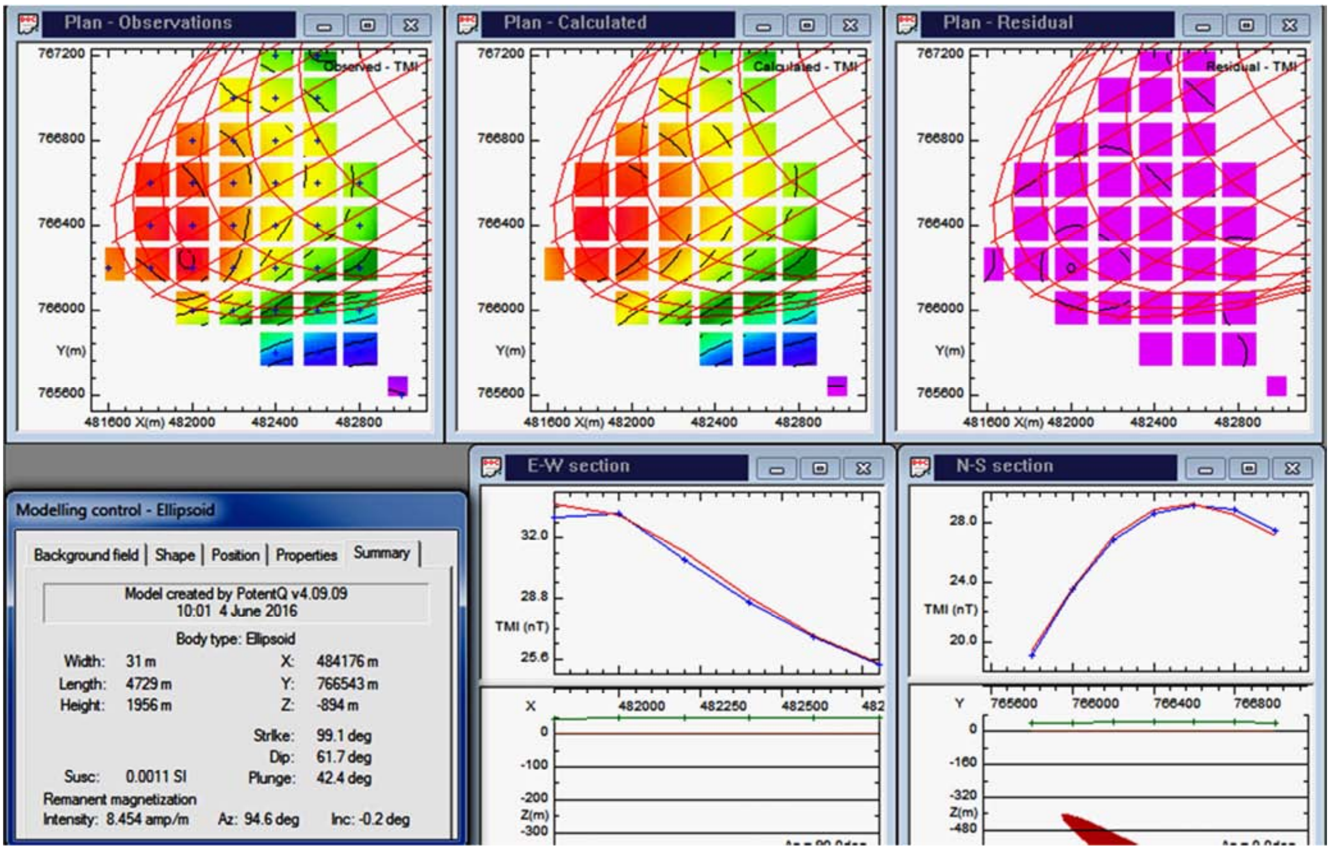

Model created by PotentQ v4.09.09
10:01 4 June 2016

Body type: Ellipsoid

Width: 31 m
Length: 4729 m
Height: 1956 m
X: 484176 m
Y: 766543 m
Z: -894 m
Strike: 99.1 deg
Dip: 61.7 deg
Susc: 0.0011 SI
Plunge: 42.4 deg
Remanent magnetization
Intensity: 8.454 amp/m
Az: 94.6 deg
Inc: -0.2 deg

Figure 17. Model result of profile 5 (P5).

Table 2. Summary of forward and inverse modelling results.

Model	Model shape	X(m)	Y(m)	Depth to anomalous body (m)	Plunge (deg)	Dip (deg)	Strike (deg)	K-value (SI)	Possible cause of anomaly
P1	Ellipsoid	455101	673417	4286	33.2	30.7	46.4	0.0400	Granite
P2	Ellipsoid	492662	688561	931	67.9	-102.5	-69.0	0.0001	Graphite
P3	Rectangular Prism	456881	709084	4654	-36.3	59.4	32.4	0.0250	Marble
P4	Rectangular Prism	475367	735433	2063	45.1	-78.0	-142.3	0.0003	Limestone
P5	Ellipsoid	484176	766543	894	42.4	61.7	99.1	0.0011	Cassiterite

5. Conclusions

The aeromagnetic data of Ogoja and Bansara areas have been interpreted qualitatively and quantitatively. The results obtained from Euler deconvolution and forward and inverse modelling techniques show clearly the variation along profiles in the surface of magnetic basement across the study area. The modelling of the residual map revealed some possible solid minerals in the study area such as graphite and cassiterite as well as rock bearing minerals such as limestone, granite and marble. Thus, the area has potentials for mineral deposits. The possible solid minerals revealed if exploited could serve as raw materials for many industries in Nigeria, thereby leading to diversification of economy of the country.

Based on the highest sedimentary thickness obtained in this work, the possibility of hydrocarbon accumulation in the area is high.

References

[1] Ofoegbu, C. O. (1984). Aeromagnetic anomalies over the Lower and Middle Benue Trough of Nigeria. J. Afr. Earth. Sci. 3: 293-296.

[2] Ofoegbu, C. O. and Onuoha, K. M. (1991). Analysis of magnetic data over the Abakaliki Anticlinorium of the Lower Benue Trough Nigeria. Marine and Petr. Geol. 8: 174-183.

[3] Onwuemesi, A. G. (1997). One dimensional spectral analysis of aeromagnetic anomalies and curie depth isotherm in Anambra Basin of Nigeria. J. Geodynamics. 23 (2): 95-107.

[4] Obi, D. A., Okereke, C. S., Obi, B. C. and George, A. M. (2010). Aeromagnetic modelling of subsurface intrusive and its implications on hydrocarbon evaluation of the Lower Benue Trough, Nigeria. European J. Sci. Res. 47 (3): 347-361.

[5] Ugwu, G. Z. and Ezema, P. O. (2012). Forward and inverse modelling of aeromagnetic anomalies over Abakaliki and Nkalagu areas of the lower Benue Trough, Nigeria. Int. Res. J. Geol. Min. 2 (8): 222–229.

[6] Ikeh, J. C., Ugwu, G. Z. and Asielu, K. O. (2017). Spectral depth analysis for determining the depth to basement of magnetic source rocks over Nkalagu and Igumale areas of the Lower Benue Trough, Nigeria. Int. J. Phys. Sci., 12 (19): 224-234.

[7] Alasi, T. K., Ugwu, G. Z. and Ugwu, C. M. (2017). Estimation of sedimentary thickness using spectral analysis of the aeromagnetic data over Abakaliki and Ugep areas of the Lower Benue Trough, Nigeria. Int. J. Phys. Sci., 12 (21): 270-279.

[8] Ugwu, G. Z., Ezema, P. O. and Eze, C. C. (2013). Interpretation of aeromagnetic data over Okigwe and Afikpo areas of the Lower Benue Trough, Nigeria. Int. Res. Geol. Min. 3 (1): 1-8.

[9] Ezema, P. O, Eze, I. D, Ugwu, G. Z. and Abdulahi U. A. (2014). Hydrocarbon and mineral exploration in Abakaliki, Southeastern Nigeria. Int. J. Engr. Sci., 3 (1): 24-30.

[10] Ofoegbu, C. O. (1985). A review of the geology of the Benue Trough of Nigeria. J. Afr. Earth Sci. 3: 285–291.

[11] Nwachukwu, S. O. (1972). The tectonic evolution of the Southern portion of the Benue Trough. Geological. Magazine, 109 (5): 411-419.

[12] Uzuakpunwa, A. B. (1974). The Abakaliki pyroclastics, Eastern Nigeria: New age and tectonic implications. Geological Magazine 111: 65-70.

[13] Olade, M. A. (1975). Evolution of Nigeria's Benue Trough (Aulacogen): A tectonic model. Geol. Magazine, 112, 576-583.

[14] Olade, MA (1976). On the genesis of the lead-zinc deposits in Nigeria's Benue rift (Alacogen): A re-interpretation. J. Min. Geol. 13 (2): 20-27.

[15] Reyment, R. A. (1965). Aspects of Geology of Nigeria, Ibadan University Press, Ibadan, Nigeria, 106.

[16] Reid, A. B., Allsop, J. M., Granser, H., Millett, A. J., Somerton, I. W. (1990). Magnetic interpretation in three dimensions using Euler deconvolution, Geophysics. 55: 80–91.

[17] Telford, W. M., Geldart, L. P., Sherriff, R. E. and Keys, D. A. (1990). Applied Geophysics, Cambridge Univ. Press, Cambridge.